Technical Note on

MIPAS-B2 Flight 6 data analysis using Oxford MWs data base selected for satellite measurements delivered on February 2001

Draft
29 JUNE 2001

Delivery of WP 7240 of the CCN#5 of the study:
"Development of an Optimised Algorithm for Routine p, T and VMR Retrieval from MIPAS Limb Emission Spectra"
Contract no. 11717/95/NL/CN

Prepared by:

Name	Institute
B.M. Dinelli	ISM-CNR

Approved by:

Name	Institute
M. Carlotti	Universita' di Bologna

Reference Documents

1. B.M. Dinelli, E. Battistini *'MIPAS-B2 data analysis'* - TN-ISM-0002
2. B.M. Dinelli, E. Battistini 'MIPAS-B2 Flight 6 data analysis with Oxford MWs data base developed for balloon measurements' - TN-ISM-0003

1. Introduction

The spectra measured by MIPAS-B2 instrument during flight 6 have been previously analysed using Occupation Matrices (OM) selected from the "old" MWs database (developed at IMK) and the new MWs selected by University of Oxford and delivered in September 2000. The results of these two analysis were reported in reference documents 1 and 2 respectively. The OMs used in the first analysis were selected from the IMK MW database using a partially automated selection tool developed at the University of Bologna. In the second analysis the OMs were selected by University of Oxford using the program MWMAKE assuming the error spectra typical of balloon measurements and a mid-latitude spring atmospheric scenario. In this selection the retrieval of atmospheric continuum was not considered.
In this technical note we report the results of a new analysis of Flight 6 measurements using the set of MWs selected by the MWMAKE program assuming the observational conditions of the MIPAS/ENVISAT experiment.

2. Occupation Matrices

The OMs used in this analysis were delivered in February 2001. These MWs have been selected using an updated version of MWMAKE where a 5-bit precision was asked for the atmospheric continuum retrieval. The selection was made considering the latitudinal and seasonal variability of the atmosphere. Tables from 1 to 6 show, for all target quantities, the list of the MWs selected for MIPAS/ENVISAT. The last two columns of these tables show the availability of each MW in flights 6 and 7 respectively. It is clear that the new set of MWs could not be used for the analysis of Flight-7, since all but one of the MWs selected for the p,T retrieval fall outside the frequency range of MIPAS-B2 during that flight. In the case of Flight 6 instead, the majority of the MWs can be used, even if for p,T retrieval some problem may arise because most of them are in a region where calibration problems are present (those MWs are marked with a ? in the corresponding column of table 1).

Table 1 – list of satellite MWs delivered in February for p,T retrieval

MW number	name	Frequency range		Flight 6	Flight 7
1	pt___ox1_001	686.400	689.400	YES(?)	NO
2	pt___ox1_017	696.200	698.375	YES(?)	NO
3	pt___ox1_003	724.700	725.400	YES(?)	NO
4	pt___ox1_009	725.600	725.675	YES(?)	NO
5	pt___ox1_004	728.300	729.125	YES(?)	NO
6	pt___ox1_008	736.200	739.175	YES(?)	NO
7	pt___ox1_006	741.975	742.250	YES(?)	NO
8	pt___ox1_007	749.350	749.500	YES(?)	NO
9	pt___ox1_002	791.375	792.875	YES	YES
10	pt___ox1_005	1073.950	1074.925	YES	NO

Table 2 – list of satellite MWs delivered in February for H_2O retrieval

MW number	name	Frequency range	Flight 6	Flight 7	MW number
1	h2o__ox1_002	807.850	808.450	YES	YES
2	h2o__ox1_011	1574.800	1577.800	NO	YES
3	h2o__ox1_008	1608.875	1609.575	YES	YES
4	h2o__ox1_010	1616.400	1616.800	YES	YES
5	h2o__ox1_009	1637.550	1637.625	YES	YES
6	h2o__ox1_007	1645.525	1646.200	YES	YES
7	h2o__ox1_007	1645.525	1646.200	YES	YES
8	h2o__ox1_001	1650.025	1653.025	YES	YES

Table 3 – list of satellite MWs delivered in February for O_3 retrieval

MW number	name	Frequency range	Flight 6	Flight 7	MW number
1	o3___ox1_013	1039.375	1040.325	YES	NO
2	o3___ox1_012	1073.800	1076.800	YES	NO
3	o3___ox1_007	1086.800	1087.550	YES	NO
4	o3___ox1_014	1112.750	1115.750	YES	NO
5	o3___ox1_001	1122.800	1125.800	YES	NO

Table 4 – list of satellite MWs delivered in February for HNO_3 retrieval

MW number	name	Frequency range	Flight 6	Flight 7	MW number
1	hno3_ox1_004	774.900	775.050	YES	YES
2	hno3_ox1_001	876.375	879.375	YES	YES
3	hno3_ox1_006	885.100	888.100	YES	YES
4	hno3_ox1_012	895.675	898.675	YES	YES
5	hno3_ox1_003	1324.175	1327.175	YES	YES

Table 5 – list of satellite MWs delivered in February for CH_4 retrieval

MW number	name	Frequency range	Flight 6	Flight 7	MW number
1	ch4__ox1_003	1155.250	1156.800	YES	YES
2	ch4__ox1_007	1169.300	1169.800	YES	YES
3	ch4__ox1_017	1215.875	1216.575	YES	YES
4	ch4__ox1_012	1227.175	1230.175	YES	YES
5	ch4__ox1_015	1236.550	1237.525	YES	YES
6	ch4__ox1_013	1247.775	1248.650	YES	YES
7	ch4__ox1_004	1255.450	1256.150	YES	YES
8	ch4__ox1_005	1256.675	1257.650	YES	YES
9	ch4__ox1_001	1350.875	1353.875	YES	NO

Table 6 – list of satellite MWs delivered in February for N_2O retrieval

MW number	name	Frequency range	Flight 6	Flight 7	MW number
1	n2o__ox1_019	1164.775	1165.075	YES	YES
2	n2o__ox1_012	1233.275	1236.275	YES	YES
3	n2o__ox1_015	1256.025	1256.275	YES	YES
4	n2o__ox1_004	1256.675	1257.975	YES	YES
5	n2o__ox1_005	1262.350	1263.125	YES	YES
6	n2o__ox1_007	1263.350	1263.900	YES	YES
7	n2o__ox1_008	1265.750	1266.800	YES	YES
8	n2o__ox1_006	1266.825	1267.750	YES	YES
9	n2o__ox1_001	1272.050	1275.050	YES	YES
10	n2o__ox1_016	1284.925	1285.975	YES	YES

Table 7 – list of satellite MWs delivered in February for NO_2 retrieval

MW number	name	Frequency range	Flight 6	Flight 7	MW number
1	no2__ox1_002	1606.775	1607.200	YES	YES
2	no2__ox1_001	1607.275	1610.275	YES	YES
3	no2__ox1_008	1612.800	1613.700	YES	YES
4	no2__ox1_003	1613.725	1616.600	YES	YES
5	no2__ox1_010	1619.125	1622.125	YES	YES
6	no2__ox1_013	1622.550	1623.475	YES	YES
7	no2__ox1_006	1624.800	1627.800	YES	YES
8	no2__ox1_004	1634.225	1634.925	YES	YES

3. Retrievals

Cross-section Look-Up Tables (LUTs) and Irregular Grids were provided for the new set of MWs and used in the forward model calculations. The OMs delivered with the MWs have been built for the tangent altitudes of the new nominal sequence of MIPAS/ENVISAT observations that no longer coincide with the tangent altitudes of the balloon measurements. Therefore, in this analysis, new Oms have been built following the rule that a MW is included in the retrievals at the tangent altitudes where there is at least one unmasked spectral point in the MW. The initial guess profiles were the same used in the final analysis reported in reference 2. It should be noted that the initial guess profile of water was the one obtained in a previous analysis of flight 6.
The χ-test values obtained in the present analysis are reported in Table 8 together with the values predicted by the MW generating algorithm. The comparison of the final χ-test values with the predicted values shows some discrepancies. In particular p,T, ozone and CH_4 χ-test values are lower than predicted. This is probably due to the fact that some systematic errors are overestimated in the MWs selection. Water, HNO_3 and NO_2 χ-test values are instead higher than predicted. HNO_3 high value is due to spectroscopic errors that have been already identified by J.M. Flaud and will be corrected in a new version of the spectroscopic database. The high χ-test value of water can be due either to spectroscopic errors or to the presence of water in the instrument during flight 6 that caused calibration problems in the MWs where strong water lines were present.

Table 8 – predicted and retrieved χ-test values of the retrievals.

	Predicted χ-test	**Retrieval χ-test**
PT	**76.4**	**23.3**
H_2O	**10.1**	**19.0**
O_3	**27.8**	**8.5**
HNO_3	**2.4**	**13.5**
CH_4	**16.5**	**4.9**
N_2O	**4.1**	**3.7**
NO_2	**2.6**	**9.1**

Figure 1 shows the tangent altitude corrections and Figure 2 reports the temperature profile obtained in this analysis. Figure 3 shows the comparison between the temperature profile of Fig.2 and those obtained with the two OMs that have been previously used for flight 6 retrievals (see Sect. 1). The three temperature profiles in Fig. 3 appear in good agreement while the altitude corrections in Fig. 4 differ for the different OMs. This may be explained by the fact that each MW is affected in a different way by systematic errors, and in p,T retrievals, some of the systematic effects tend to be compensated by the pointing parameters. Moreover, since the nominal error on the pointing is of the same order of magnitude of the random errors of the retrieval, even the use of the a priori information on the Line-Of-Sight does not help to constrain the retrieval.
Figures from 5 to 9 show the VMR profiles retrieved in the present analysis together with those obtained with the two OMs that have been previously used for flight 6. On the average the agreement is poor. A further retrieval test was carried out for VMR retrievals with the two Oxford OMs. In this test the nominal values were used for pointing and climatological profiles were used for temperature and pressure. The VMR profiles retrieved in this test are in very good agreement between themselves. This indicates that the differences found in the full retrieval chain are mainly due to the different results of the p,T retrievals.

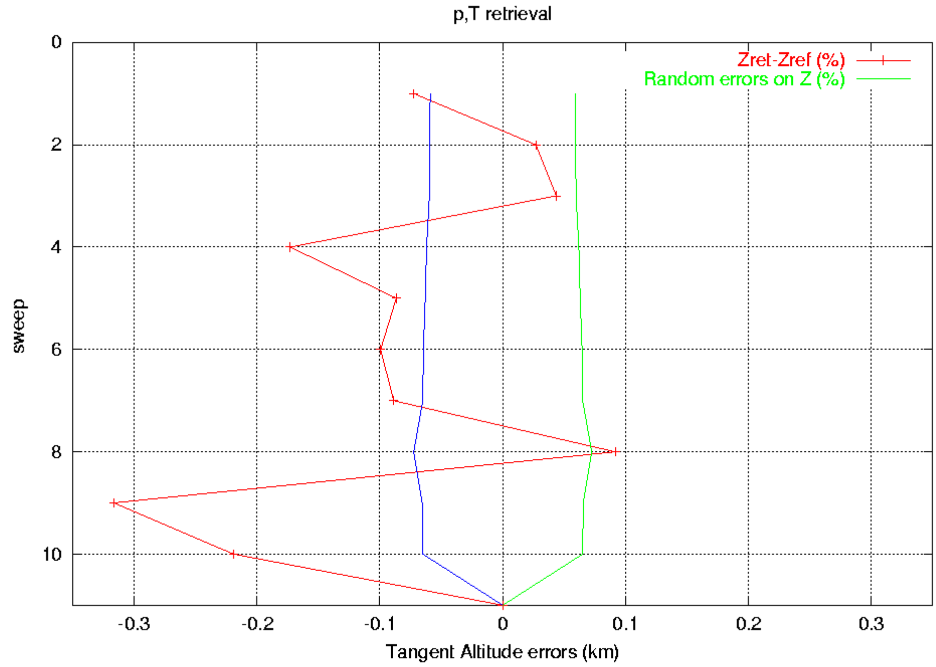

Figure 1 Altitude corrections obtained in the present analysis

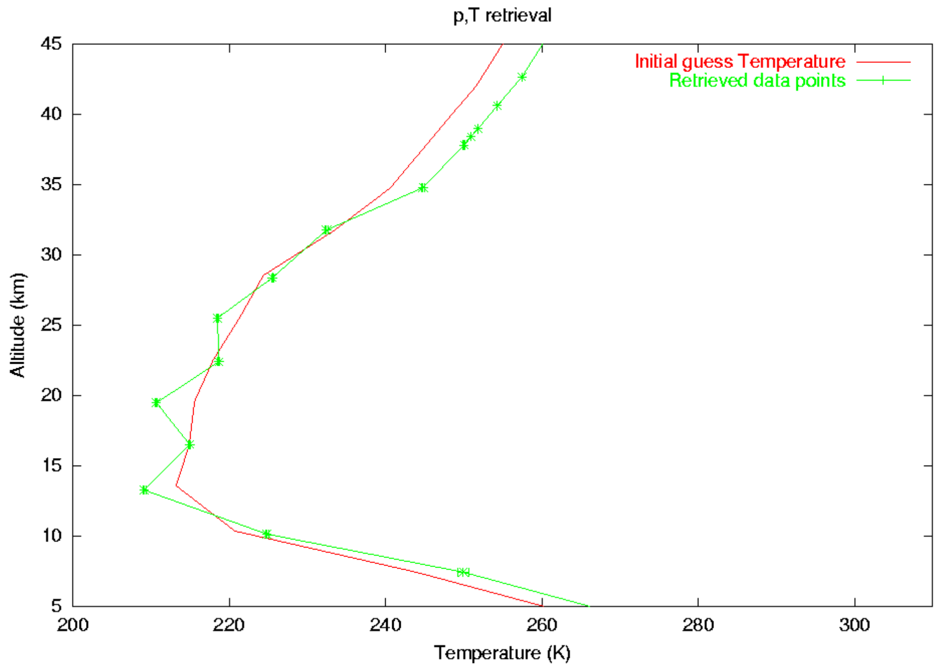

Figure 2 Temperature profile obtained in the present analysis

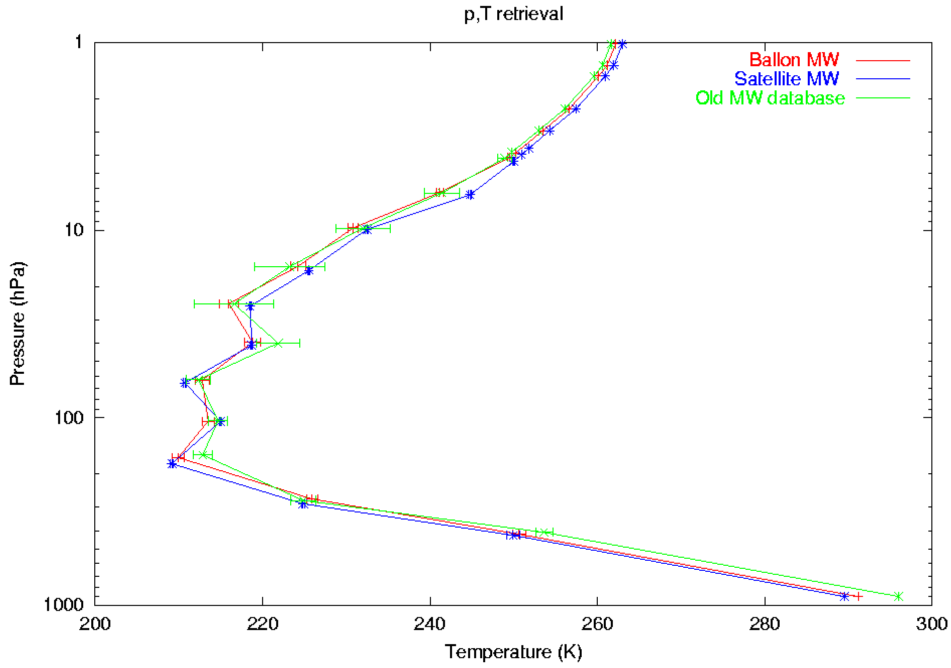

Figure 3 Comparison of the temperature profiles obtained using the three different MW databases

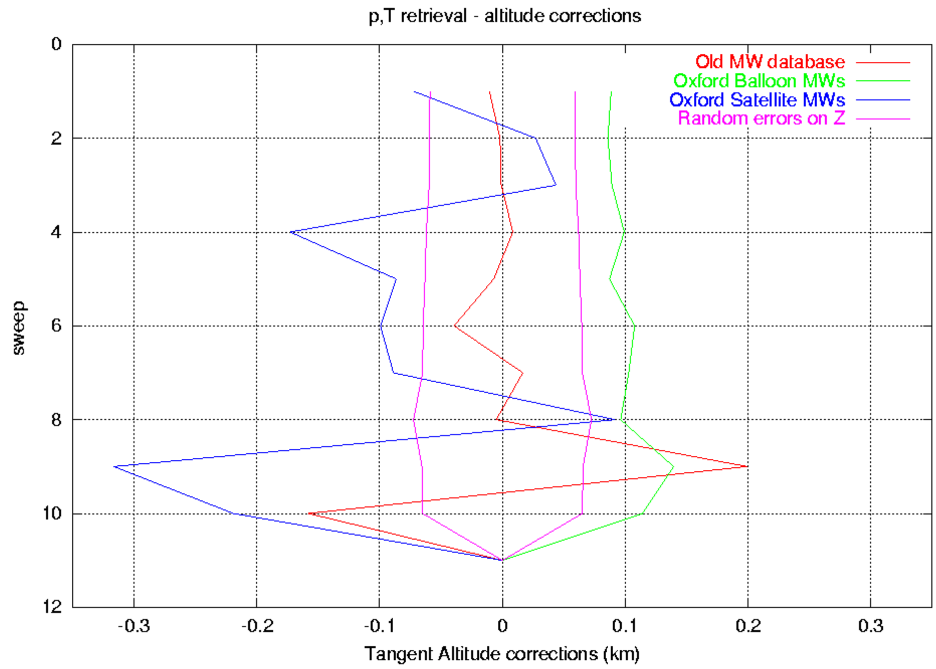

Figure 4 Comparison of the tangent altitude corrections obtained using the three different MW databases

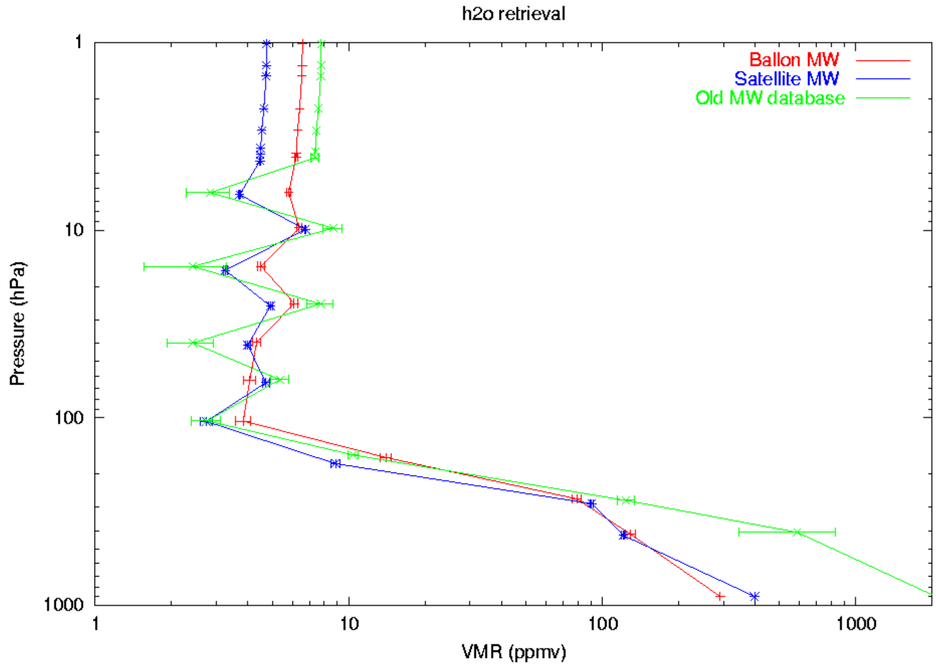

Figure 5 Comparison among the Water VMR profiles obtained using the three different MW databases

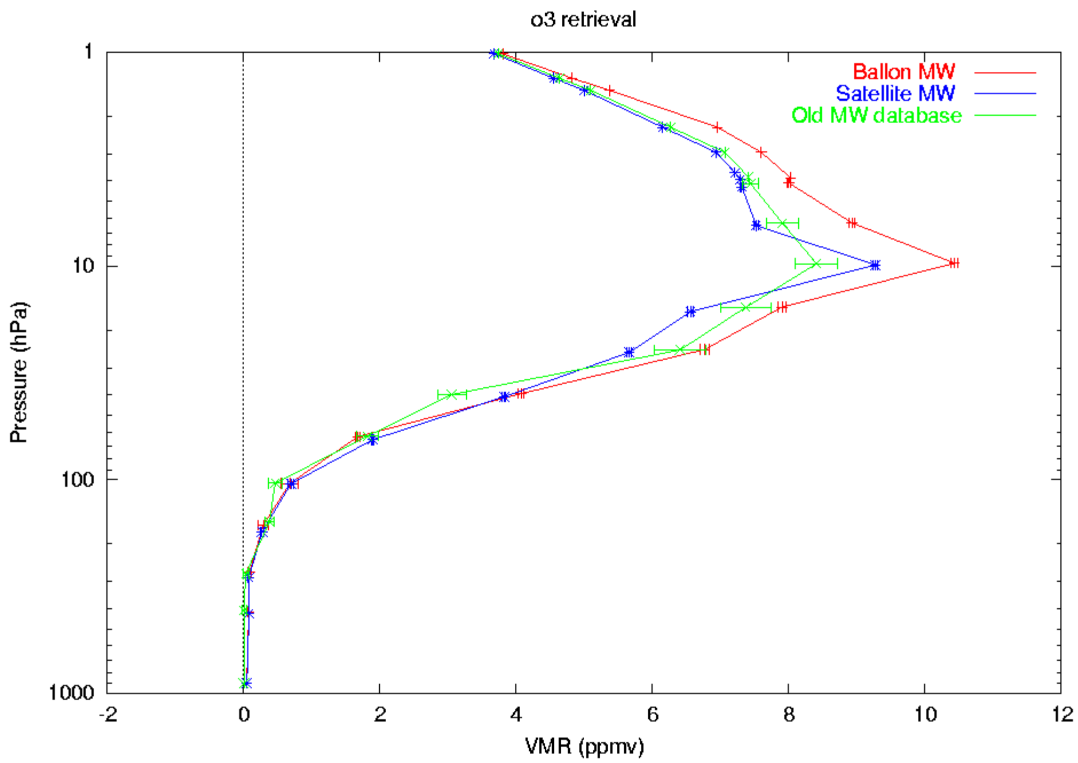

Figure 6 Comparison among the three Ozone profiles obtained using the three different MW databases

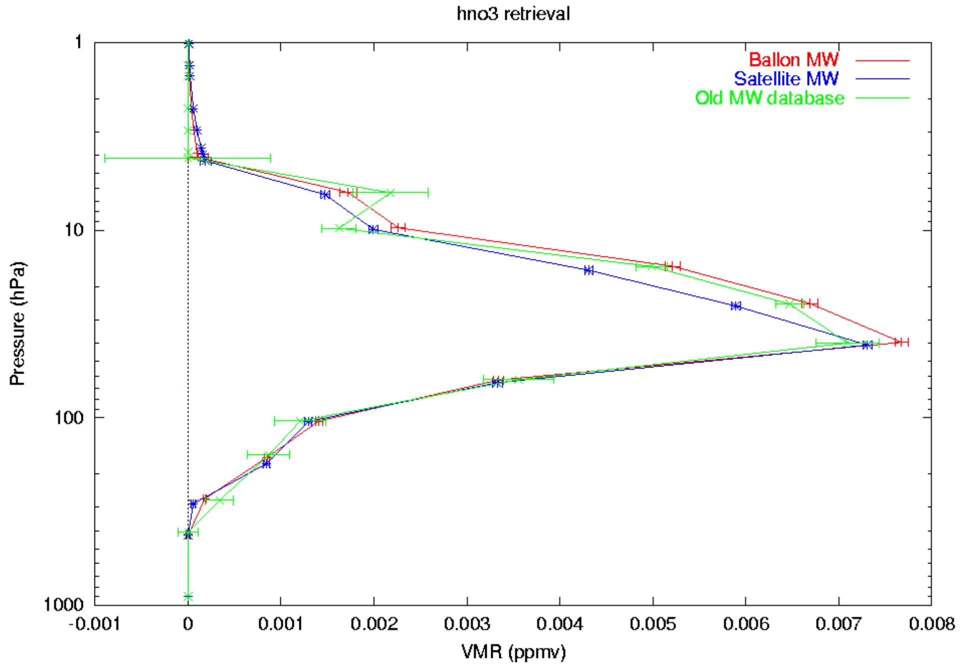

Figure 7 Comparison among the three HNO_3 profiles obtained using the three different MW databases

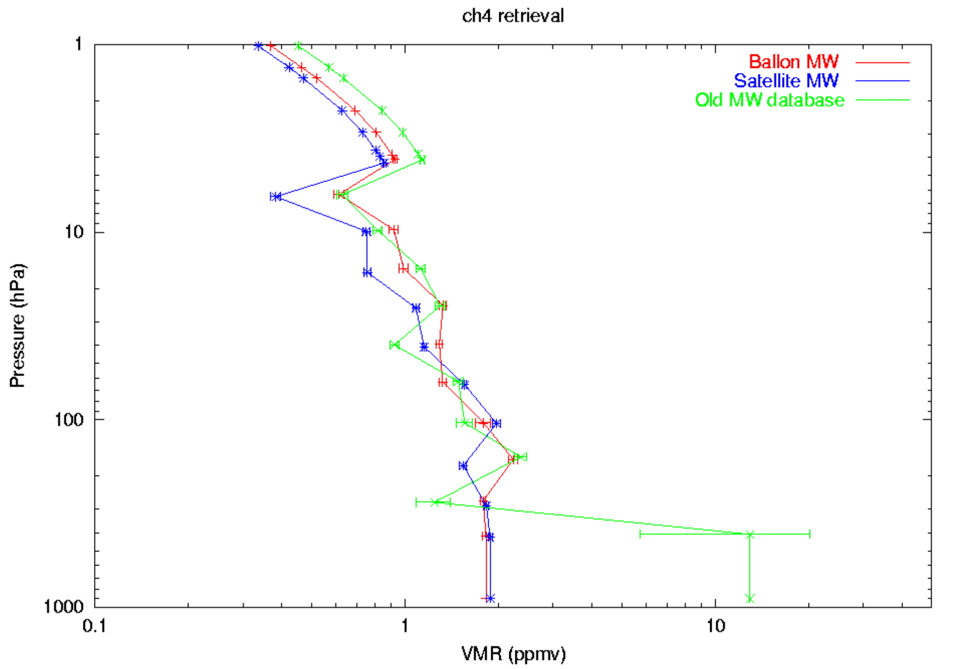

Figure 8 Comparison among the three CH_4 profiles obtained using the three different MW databases

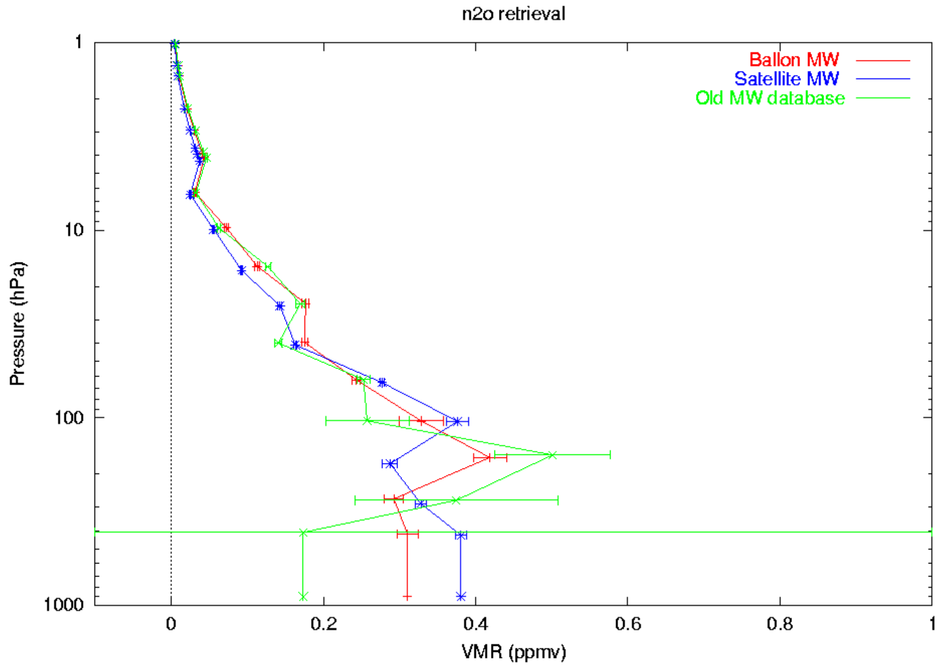

Figure 9 Comparison among the three N_2O profiles obtained using the three different MW databases

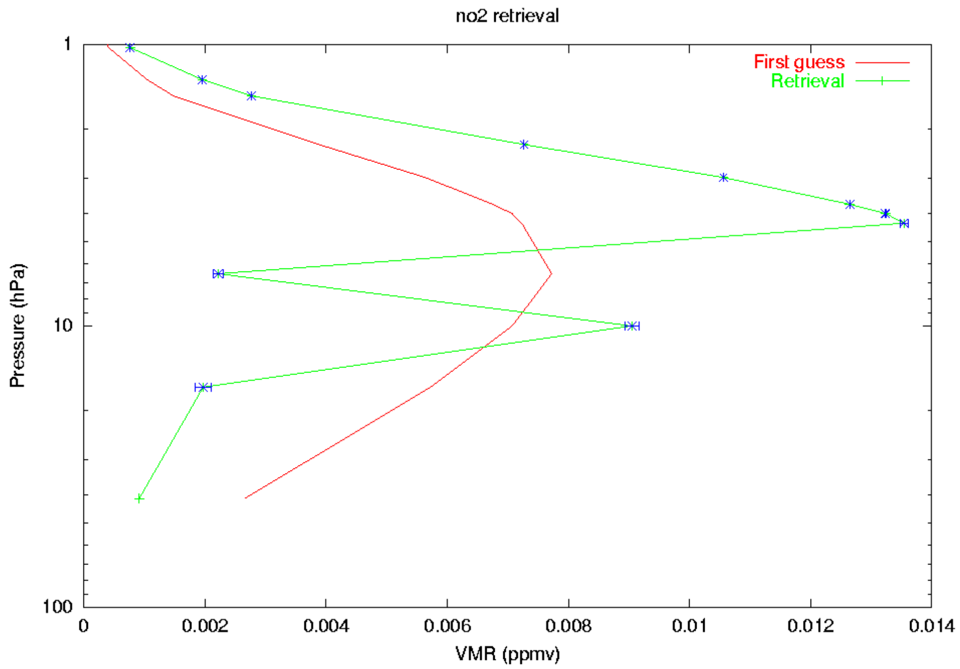

Figure 10 Initial guess (red) and retrieved (green) NO_2 profile

Figure 10 reports the VMR profile of NO_2 retrieved in this analysis. This represents the first profile determined, from MIPAS-B measurements for this molecule. It can be seen in figure 10 that the retrieval is not stable. On the other hand the χ-test value for the NO_2 retrieval is higher than predicted (see Table 2). The residuals of NO_2 retrieval suggest that we are in presence of some spectroscopic errors. Recently Flaud and Piccolo found a missing molecule (O_2) in the list of the absorbers for which LUTs have been computed for NO_2 MWs. This may be the cause of the poor quality of this retrieval.

3.1 Final remarks

In general the ESDs of the retrievals are similar to those obtained using the Oxford OMs selected for balloon data. As before, strong water lines are never reproduced correctly (probably due to calibration errors) causing the final χ-test value to be higher than predicted.
The retrieved VMRs are sometime different from those retrieved using the balloon MWs or the IMK MWs. This difference cannot be explained by the measurement noise. However, when using the same pointing and atmospheric pressure and temperature profiles, the differences almost disappear. This suggests that the differences in the VMRs results is mainly due to the differences in the p,T retrieval. Unfortunately, the OMs selected by University of Oxford for the satellite measurements do not provide a satisfactory performance in the p,T retrieval of balloon measurements. In particular, the final tangent altitude corrections are quite high. This poor performance can be attributed to systematic errors that affect the MIPAS-B measurements but are not properly evaluated when selecting the MWs. This explanation is supported by the comparison between theoretical and retrieved χ-test values.

4. Problems encountered with the satellite MWs

Table 3 shows, as an example of the average situation, the spectral mask corresponding to a MW selected for the p,T retrieval. In this table the "TRUE" spectral points are marked with a black rectangle, the "FALSE" are marked with an open rectangle. On the average, the "FALSE" points are about 58% of total for the MWs of p,T and water retrievals, while they are about 36% for the other retrievals. It can be seen in Table 3 that the grid of the "TRUE" points can be rather sparse.

Table 3. Spectral mask for a MW for p,T retrieval

Alt.	MASK
33.7	□□■□■■■■■□□□□□□□□□□□□□□■■■■□□□■■□□□■■□□□□□□□□□□□□□□□□□□□□□□□■
28.5	□□□□■□□□■□□■■□□■□□□□□□■■■■■□□□□■■□□□□□□□■□□□□□□□□□□□■□□□□□□□
25.6	□□□□□□□□□□□■■□□■□□□□□■■■□■■□□□□□■□□□□□■■■□□□□□□□□□□□■■■■□□■■
22.5	■□□□■□□□■□□□■□□■□□□□□■■■□■■□□□□□□□□□□■□■■■□□□□□□□□□□□□□■■□□□
39.6	■□□□■□□□■□□□■□□■□□□□□■■■□□□□□□□□□□□□□■□□□□□□□□□□□□□□□□□■□□□□
36.4	□□□■■□■■■■■■■□□■□□■■■■■□□□□□□□□□□□□□□□□□□□□□□□□□□□□□□□□□□□□□
33.6	□□□■■□■■■■■■■□□■□□■■■■■□□□□□□□□□□□□□□□□□□□□□□□□□□□□□□□□□□□□□
30.3	□□□□□□■■■■■■■■■■■□■■■■■□□□■■■□□□□□■□□■■■■■■■□■■■■□□□□■□□□□□□□
7.4	□□■□□□■■■■■■■■■■■■■■■■■□□□■■□■■□□■■□□■■■■■■■□■■■■□■□□■□□□□□□□

Since the IGs are optimised for the "TRUE" points only, the visual inspection of the residuals resulted to be very hard. This situation could cause problems during the commissioning phase when many of the diagnostic tools are based on the behaviour of the residuals. Figure 11 shows plots relative to the above MW when used at the tangent altitude of ~ 32 km in the retrieval. In this figure (as well as in all the following figures) the blue line identifies the measured spectrum and the red line the spectrum simulated at convergence of the retrieval process. On the simulated spectrum of Fig. 11 the "TRUE" points are marked in green. The straight brown lines around the zero mark the +/- noise level for this MW. The orange line represents the difference between observation and simulation (residual) with marked in green the "TRUE" points. The red crosses at the very bottom of the figure mark the frequency position of the main isotope of the main-gas transitions (CO_2 in this case) while the yellow bars show their relative intensity computed at 250 K. It can be seen in Fig. 11 that, at the high frequency end of the MW, the simulation and the measurement are quite different, suggesting some error either in the spectroscopy or in the contaminant VMR profiles. After a thorough analysis at University of Oxford it has turned out that the difference is just caused by the not optimised IG in that region.

For some MWs the frequency extension and the distribution of "TRUE" points lead to compute the full radiative transfer for a wide MW that, afterwards, is used only in a few unmasked points laying at the edges and the MW shown in fig. 11 is also a good example for this.

In the present analysis spectroscopic errors in some MWs have been found. As an example, in Figure 12 we show the HNO_3 MW HNO3_006 where this problem is evident.

The sparseness of the "TRUE" in the spectral masks makes the atmospheric continuum difficult to determine in some MWs. An example of MW where this problem was encountered is provided in Figure 13.

In some MWs "TRUE" points fall on strong transitions that do not belong to the target molecule. An example of this problem is provided in Figure 14 that refers to a MW selected for NO_2. In this figure the spectral feature at 1609.45 cm^{-1} does not belong to NO_2 but "TRUE" points fall on it (this is a possible cause for the high χ-test value found in the NO_2 retrieval).

In many MWs the central part of the spectral lines of the target species is masked; this avoids systematic effects due to saturation. This is not the case shown in figure 15 where an HNO_3 MW is represented. In this figure it can be seen that a whole band of HNO3 is masked even if it clearly is not saturated.

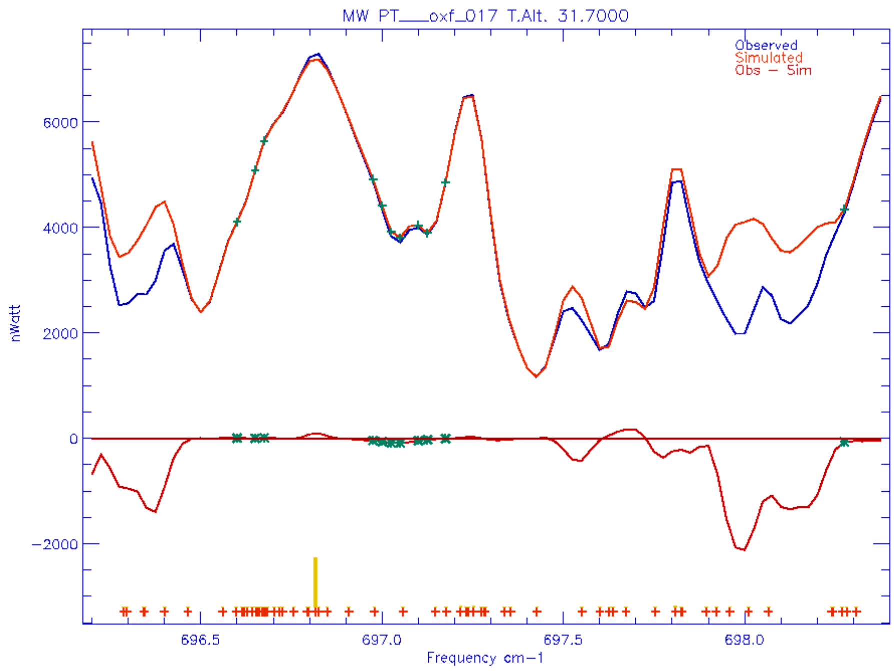

Figure 11 MW PT_0017 at tangent altitude 31.7 km

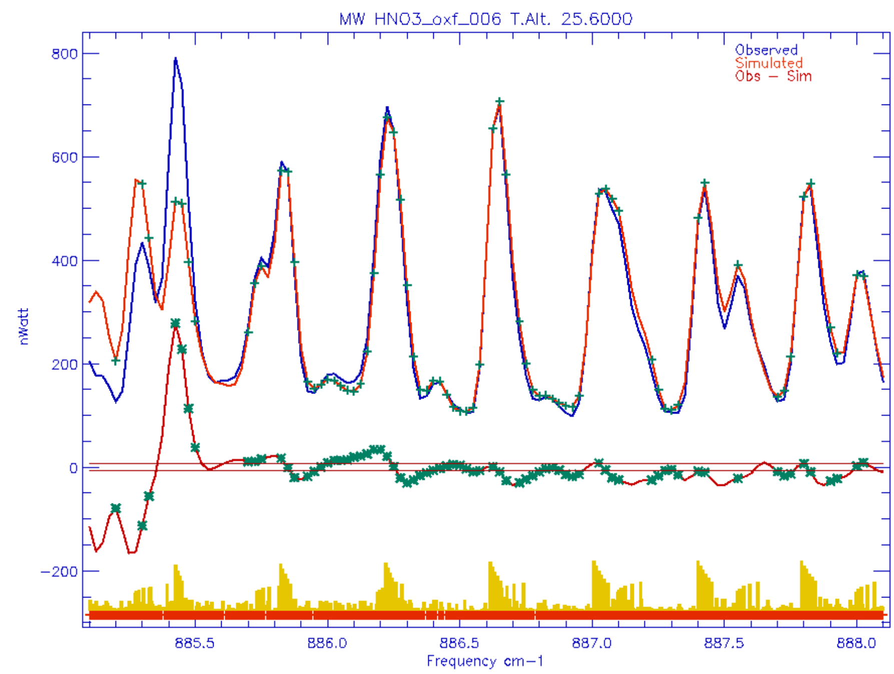

Figure 12 MW HNO3_0006 at the tangent altitude of 25.6 km

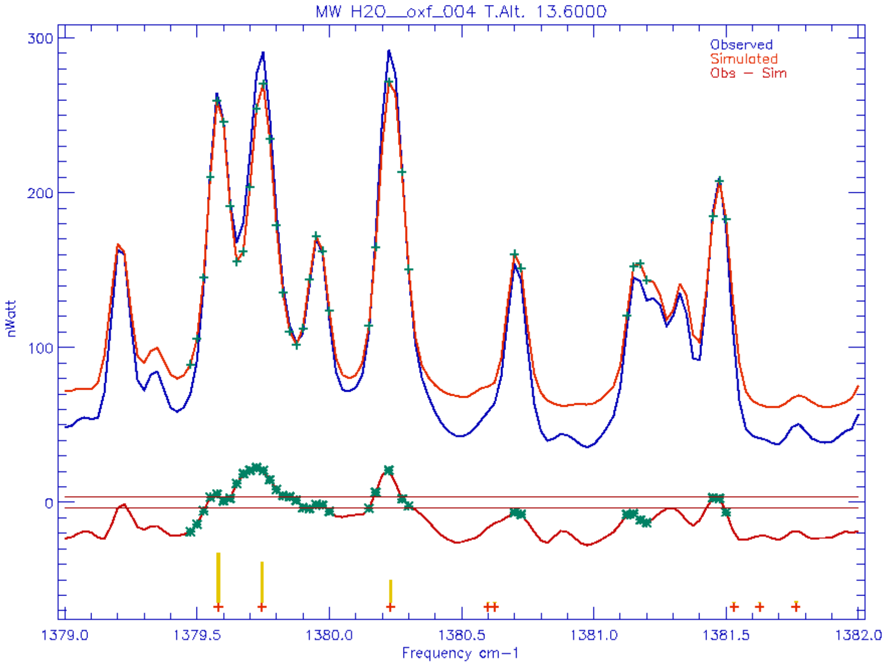

Figure 13 MW H2O_004 at the tangent altitude of 13.6 km

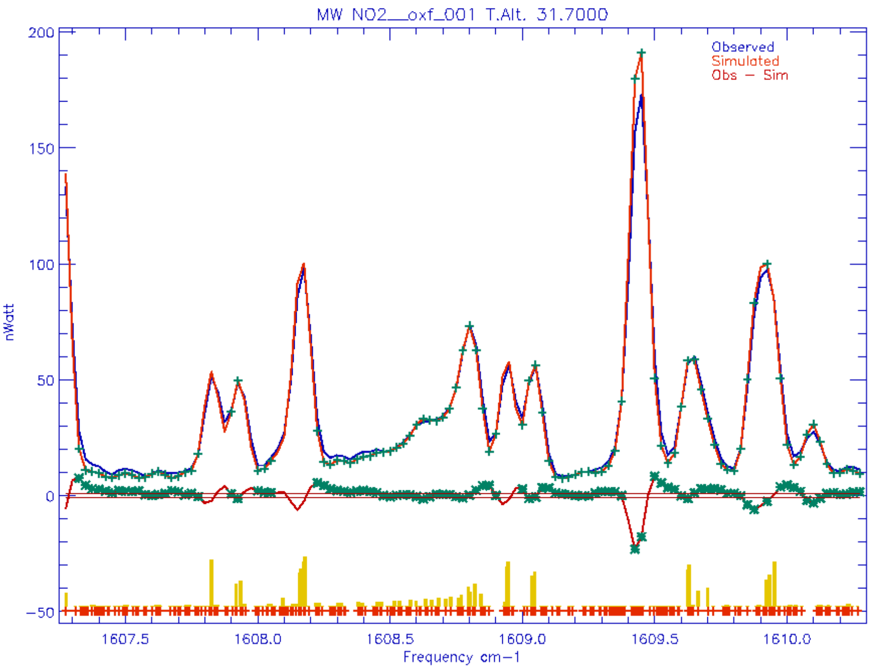

Figure 14 MW NO2_001 at the tangent altitude of 31.7 km

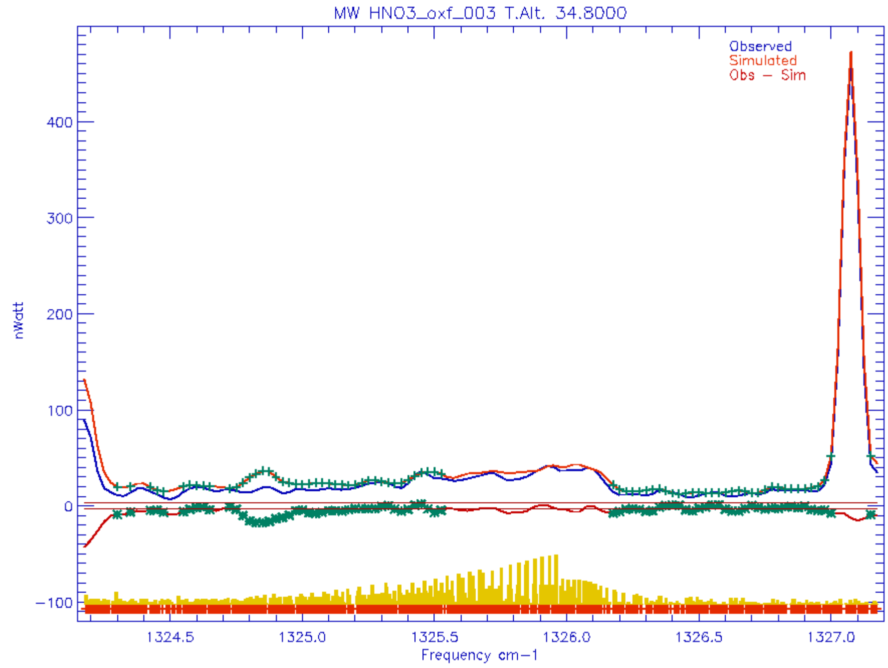

Figure 15 MW HNO3_003 at the tangent altitude of 34.8 km